Design and Implementation of True Random Noise Radar System

Woo-Ki Min[1] · Cheol-Hoo Kim[1] · Constantin A. Lukin[2] · Jeong-Phill Kim[1]

Abstract

The design theory and experimental results of a true random noise radar system are presented in this paper. Target range information can be extracted precisely by correlation processing between the delayed reference and the signal received from a target, and the velocity information by the Doppler processing with successive correlation data. A K-band noise radar system was designed using random FM noise signal, and the characteristics of the fabricated system were examined with laboratory and outdoor experiments. A C-band random FM noise signal was generated by applying a low-frequency white Gaussian noise source to VCO(Voltage Controlled Oscillator), and a K-band Tx noise signal with 100 MHz bandwidth was obtained by using a following frequency multiplier. Two modified waveguide horn arrays were designed and fabricated, and used for the Tx and Rx antennas. The required amount of Tx/Rx isolation was attained by using a coupling cancellation circuit as well as keeping them apart with predetermined spacing. A double down-conversion scheme was used in the Rx and reference channels, respectively, for easy post processing such as correlation and Doppler processing. The implemented noise radar performance was examined with a moving bicycle and a very high-speed target with a velocity of 150 m/s. The results extracted by the Matlab simulation using the logging data were found to be in a reasonable agreement with the expected results.

Key words : Noise Radar, True Random Signal, Correlation, FFT, Range, Doppler, LPI, Ambiguity.

I. Introduction

Recently much more accurate 3-dimensional target information has been required in radar systems with outstanding capabilities such as high resolution, LPI(Low Probability of Intercept), strong immunity against hostile jamming and nearby unwanted interference, and simultaneously unambiguous measurement in the range and Doppler domain. However, these requirements cannot be easily met with conventional radar signals such as periodic pulse or FM signals. As an alternative, pseudo-random noise signals have been intensively studied, but problems of ambiguity and extra work for code assignment remain unsolved. For the ultimate solution, increasing attention has been paid to true random noise radar, and it is known to have all of the previously mentioned attractive features.

The theoretical work on distance measuring using a true random noise signal was done by Horton in 1959[1], but its development proceeded slowly due to immature techniques and the limited availability of suitable electronic components. However, along with the progress of a wideband noise signal generator, high-speed and high-density digital hardware, and digital signal processing algorithms, the realization of a noise radar system has come true.

Some research activities have been devoted to the development and implementation of random noise radar over the past few years for applications such as ultra-wideband SAR/ISAR imaging, foliage penetration, Doppler sensor and polarimetry, and collision warning[2]~[7]. However, since the considerable related research results are kept secret, it is not easy to find out information on the detailed design theory and implementation technology.

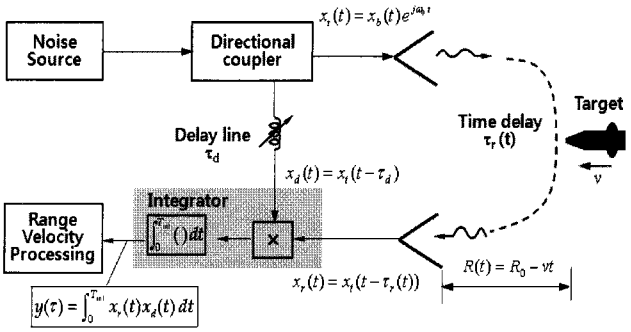

Fig. 1. Block diagram of true random noise radar system.

This paper deals with the detailed design theory and procedure of a random noise radar system. Even though the theory of operation is relatively well known[1]~[7], a brief introduction is made to help readers understand the subsequent detailed design theory. Based on the design theory, a K-band noise radar system is designed and implemented, and its performance is examined with experi-

Manuscript received June 30, 2009 ; revised September 7, 2009. (ID No. 20090630-027J)
[1]School of Electrical and Electronics Engineering, Chung-Ang University, Seoul, Korea.
[2]LNDES, IRE NASU, Ukraine.

ments: one with a moving bicycle and the other with a small high-speed target. The target's range and Doppler information are extracted by correlation and Doppler processing.

Ⅱ. Theory of Operation

2-1 Basics of True Random Noise Radar

Fig. 1 shows the simplified block diagram of true random noise radar. The true random noise signal transmitted via a Tx antenna can be expressed in the complex form as

$$x_t(t) = x_b(t)e^{j\omega_0 t} \tag{1}$$

where $x_b(t)$ denote the baseband noise signal whose signal bandwidth is B and ω_0 is the carrier angular frequency. The delayed reference signal and received signal from a target which is assumed to approach with a radial velocity v, can be expressed as

$$x_d(t) = x_b(t-\tau_d)e^{j\omega_0(t-\tau_d)} \tag{2}$$

$$x_r(t) = x_b((1+\alpha)t-\tau_0)e^{j\omega_0((1+\alpha)t-\tau_0)} \tag{3}$$

where τ_d denotes the specified time delay in the reference channel. The initial delay time(τ_0) and compression factor(α) for a moving target are given as

$$\tau_0 = \frac{2R_0}{c}, \quad \alpha = \frac{2v}{c}. \tag{4}$$

The speed of light in free space is denoted by c.

After the received and delayed reference signals are down converted, their correlation integral can be obtained by integrating their multiplication result during the specified integration time T_{int} as

$$C(\tau,\alpha,t) = \frac{1}{T_{\text{int}}}\int_{T_{\text{int}}} x_b^*(t)x_b(t+\alpha t-\tau)e^{j2\pi(\alpha t-\tau)}dt \tag{5}$$

where $\tau\ (=\tau_0-\tau_d)$ means the delay difference of two signals and the superscript "*" means taking a complex conjugate. Since $x_b(t)$ is a random signal, it is known that the value $C(\tau, \alpha, t)$ becomes not a constant but a function of the start time of integration. Therefore, only the following expectation value is meaningful:

$$\begin{aligned} E[C(\tau,\alpha,t)] &= \frac{1}{T_{\text{int}}}\int_{T_{\text{int}}} E\left[x_b^*(t)x_b(t+\alpha t-\tau)\right]e^{j2\pi(\alpha t-\tau)}dt \\ &= \frac{1}{T_{\text{int}}}\int_{T_{\text{int}}} R_b(\alpha t-\tau)e^{j2\pi(\alpha t-\tau)}dt \end{aligned} \tag{6}$$

where $R_b(.)$ denotes the autocorrelation function of $x_b(t)$. For the special case of a fixed target, the expectation becomes simplified as $E[C(\tau,\alpha=0,t)] = R_b(\tau)$.

From the Wienner-Kintchin theorem[8], it is well known

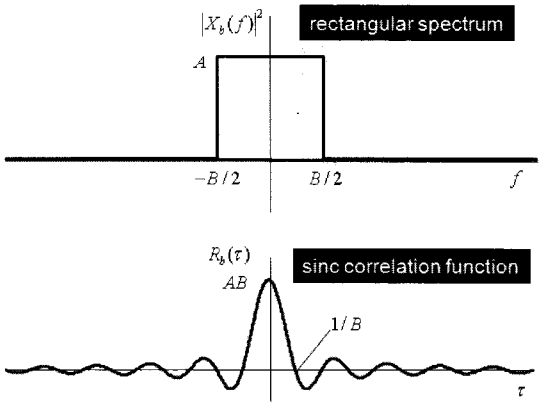

Fig. 2. Relation between a rectangular power spectral density and its correlation function.

that there is a Fourier transform relation between the correlation function $R_b(\tau)$ and its power spectral density function $|X_b(f)|^2$ in the τ- and f-domains. The correlation function of a signal having a rectangular power spectrum with a bandwidth of B becomes a sinc function ($R_b(\tau) = B\text{sinc}(B\tau)$) as shown in Fig. 2, and a 3-dB correlation width $\Delta\tau$ in the delay-time domain is approximately given as the inverse of the bandwidth B as $\Delta\tau \simeq 1/B$. This means that high-resolution capability can be obtained with a wideband probing signal.

2-2 Range Processing

A peak value is known to be observed in the correlation integral for a fixed target at τ=0(τ_d=τ_0). This condition can be met by adjusting τ_d, and target range information can be extracted by measuring such a τ_d. The range is calculated as

$$R = \frac{c\tau_d}{2} \tag{7}$$

For a moving target, αf_0 becomes the Doppler frequency ($\alpha f_0 = (2v/c)f_0 = f_D$), and the maximum output of the correlation integral becomes slightly less than that for a fixed target. This can be regarded as a degradation related to the amount of the Doppler frequency(Doppler mismatch loss). However, it can be restored when the Doppler tracking technique is used. In the most applications, since α becomes so small it can be ignored for the range processing, the range information can be obtained by measuring τ_d as in the case of a fixed target.

2-3 Doppler Processing

Now let us turn our attention to Doppler processing. One way is the Doppler tracking method as mentioned before. In this case, α can be interpreted as the quantity

related to the Doppler difference, and the maximum correlation output is expected when $\alpha t-\tau=0$ holds, that is, when the tracking conditions in Doppler and the range are met perfectly($\alpha=0$ and $\tau=0$). Therefore, the velocity information can be extracted by measuring α_d at that time, and it is calculated as

$$v=\frac{c\alpha_d}{2} \tag{8}$$

An alternative method is to use lowpass filtering and the following FFT(Fast Fourier Transform) processing. For a meaningful correlation integral, the target should reside within the range bin(correlation bin) of interest during the operation of the correlation integral, that is, T_{int} should be less than or equal to a dwell time($t_{d\omega}$) as

$$T_{\text{int}} \le t_{d\omega}=\frac{\Delta R}{v}=\frac{c}{2v}\Delta\tau=\frac{c}{2vB} \tag{9}$$

Ignoring the term $e^{j2\pi f_0\tau}$ in (6) which is independent of the measurement time t, let us consider the relation between $R_b(\alpha t-\tau)$ and $e^{j2\pi\alpha f_0 t}$. First, it is known that

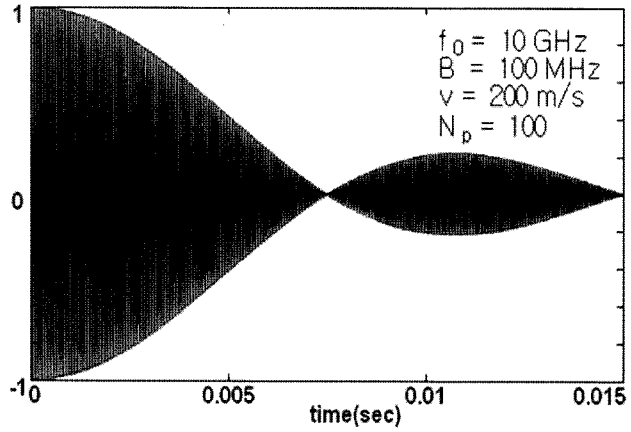

(a) Case of relatively narrow band

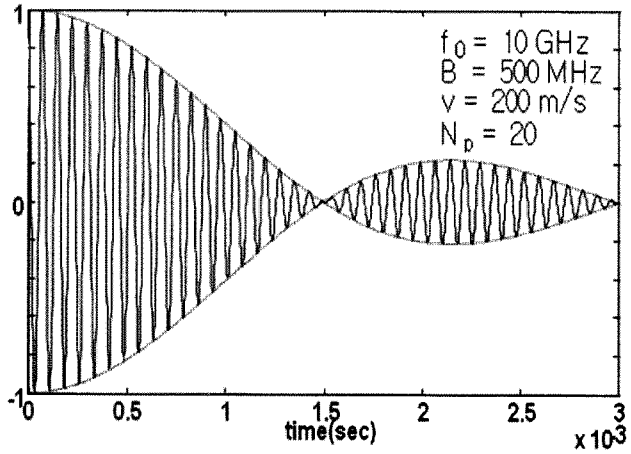

(b) Case of relatively wide band

Fig. 3. Relation between Doppler filling and fractional bandwidth.

the 3-dB pulse width(Δt) of $R(\alpha t-\tau)$ in the t-domain (measurement domain) is related to the 3-dB delay width $\Delta\tau$ as $\Delta t=\Delta\tau/\alpha$, and its expression becomes the same as the dwell time. Now the number of sinusoidal waves (the number of Doppler fillings) within Δt can be calculated as

$$N_p=f_D\Delta t=\frac{f_0}{B}=\frac{1}{FBW} \tag{10}$$

where FBW denotes the fractional bandwidth. As an example, a noise signal having a center frequency of 10 GHz and a bandwidth of 100 MHz yields N_p=100 as shown in Fig. 3(a), which is not a function of a target velocity except for the case of a fixed target. The effect of the target velocity is also reflected in the slope of the envelope in the measurement-time domain. Another case of a center frequency of 10 GHz and a bandwidth of 500 MHz is displayed in Fig. 3(b), where N_p=20. As seen in these figures, except for the case of wide fractional-bandwidth, the envelope of the integrand becomes nearly constant compared with a Doppler signal. Therefore it is acceptable to represent the correlation integral by summing its sub-integrals with the sub-correlation time($T_{sc}=T_{\text{int}}/M$) as

$$\begin{aligned}E\{C(\tau,\alpha,t)\}&=\sum_{m=1}^{M}\int_{(m-1)T_{sc}}^{mT_{sc}}R_b(\alpha t-\tau)e^{j2\pi f_0 t}dt\\&\cong\sum_{m=1}^{M}R_b(\alpha mT_c-\tau)\int_{(m-1)T_{sc}}^{mT_{sc}}e^{j2\pi f_0 t}dt\end{aligned} \tag{11}$$

and it can be further simplified by algebraic manipulation as

$$E\{C(\tau,\alpha,t)\}\cong\Psi\sum_{m=1}^{M}R_b(\alpha mT_{sc}-\tau)e^{j2\pi f_D mT_{sc}} \tag{12}$$

with $\Psi=T_{sc}\,\text{sinc}(f_DT_{sc})e^{j\pi f_DT_{sc}}$.

Now the Doppler frequency information can be extracted by the FFT processing with these successive sub-correlation data. In this case, the total number of sub-correlations becomes the number of FFT points. To extract reliable Doppler frequency information, the sub-correlation frequency($f_{sc}=1/T_{sc}$), that is, the FFT sampling frequency should be chosen to meet the Nyquist criterion[8] for the maximum expected Doppler frequency ($f_{D,\max}$) as $f_{sc}\ge 2f_{D,\max}$. This constraint can also be deduced from the term(f_DT_{sc}) in the expression of Ψ, where f_DT_{sc} <1/2 should hold for ensuring a reliable processing result.

Even though the above sub-correlation algorithm is developed for implementing a digital correlator, it can also be applied for implementing an analog correlator by replacing a sub-correlation with an LPF(Lowpass Filter) whose cut-off frequency is $f_{D,\max}$. The Doppler information can be extracted by placing an ADC(Analog-to-Di-

gital converter) whose sampling frequency is $2f_{D,\max}$ and FFT processor successively. If only a moving object is the target of interest, a BPF(Bandpass Filter) can be used instead.

2-4 Ambiguity, Resolution, and Sidelobe Characteristics

In the case of a Tx signal with a rectangular spectrum, a rather high range-sidelobe of 13 dB may cause some problems in range processing(Fig. 2). This kind of problem can be solved by using a noise signal that has a weighted spectrum, especially the Gaussian spectrum. The expressions of the Gaussian power spectrum and the corresponding correlation function are given as

$$|X_b(f)|^2 = e^{-af^2}, \qquad R_b(\tau) = \sqrt{\frac{\pi}{a}} e^{-(\pi^2/a)\tau^2} \tag{13}$$

Unlike the case of a rectangular spectrum, the bandwidth should be calculated between two frequencies at which its power spectrum density is -7.73 dB in order to guarantee a 3-dB delay width $\Delta\tau \approx 1/B$. After solving the problem of a time sidelobe with spectrum weighting, a very promising feature can be obtained, that is, no ambiguity problems in the range and Doppler simultaneously.

Now let us consider the Doppler resolution characteristics. Since it is well known that the available Doppler resolution (Δf_D) is given as the inverse of the integration time as $\Delta f_D = 1/T_{\text{int}}$, T_{int} should be chosen as

$$T_{\text{int}} \geq \frac{1}{\Delta f_D} \tag{14}$$

With the condition (9), the resulting constraint on T_{int} becomes

$$\frac{1}{\Delta f_D} \leq T_{\text{int}} \leq t_{d\omega} \tag{15}$$

From the above conditions, the following uncertainty relation between $\Delta\tau$ and Δf can be attained:

$$\Delta\tau \, \Delta f_D \geq \frac{2v}{c} \tag{16}$$

This means that $\Delta\tau$ and Δf cannot be measured with much higher resolution simultaneously. One example is that if a wider bandwidth B is chosen for the higher-resolution capability of the range resolution, then ΔR becomes smaller and it results in smaller $t_{d\omega}$, that is smaller T_{int}. Finally the Doppler resolution worsens, and vice versa.

The Non-uniform envelope $R_b(\alpha m T_{sc} - \tau)$ affects on the Doppler sidelobe and resolution characteristics. Compared to a uniform envelope, the sidelobe level becomes lower whereas the Doppler resolution capability is degraded as shown in Fig. 4. However, the amount of change is so little it can be ignored.

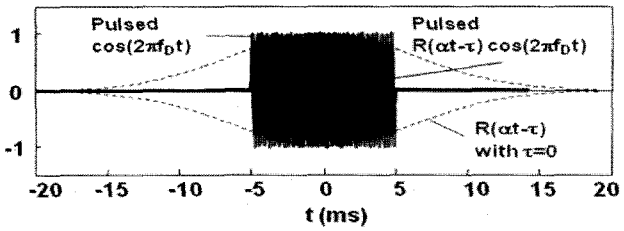

(a) Region for Doppler filtering

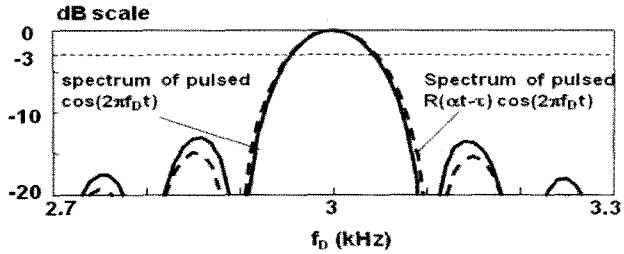

(b) Resulting Doppler processing results

Fig. 4. Degradation of Doppler resolution characteristics due to the weighting by correlation function(f_0=3 GHz, B=100 MHz, v=150 m/s, T_{int}=10 ms).

2-5 Processing Block and Algorithm

The conceptual block diagram for the range and velocity processing based on the theory described before is shown in Fig. 5. At first, appropriate numbers of delay elements are successively placed in the delayed reference channel, and the output of each delay element is multiplied with the received signal. In the analog domain, the correlator can be implemented by using a mixer and an LPF. The cut-off frequency of the LPF is generally chosen to be slightly larger than the expected maximum Doppler frequency $(f_{D,\max})$ to reduce as many interference and spurious components as possible. Now the Doppler information in the specified range bin can be extracted by the FFT processing after the LPF output is sampled with an appropriate sampling frequency of $f_{s,FFT} \geq 2f_{D,\max}$.

This operation can also be implemented in the digital domain. At first, AD sampling is performed for the final down-converted delayed-reference and received signals with a sampling frequency of $f_s \geq 2B$. Digital delay elements(D-flip flops) with a delay time of $1/B$ are placed successively, the output of each delay element and Rx digital data are multiplied, and the output is accumulated for a sub-correlation time of $T_{sc}(=1/f_c) \leq 1/2f_{D,\max}$ as depicted in Fig. 6. This means that the number of data points for each sub-correlation(accumulation) becomes $N_{sc} \leq f_s T_{sc}$. Now gathering the accumula-

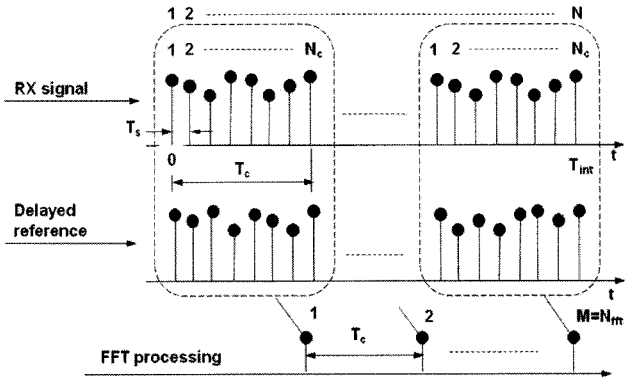

(a) Concept of sub-correlation

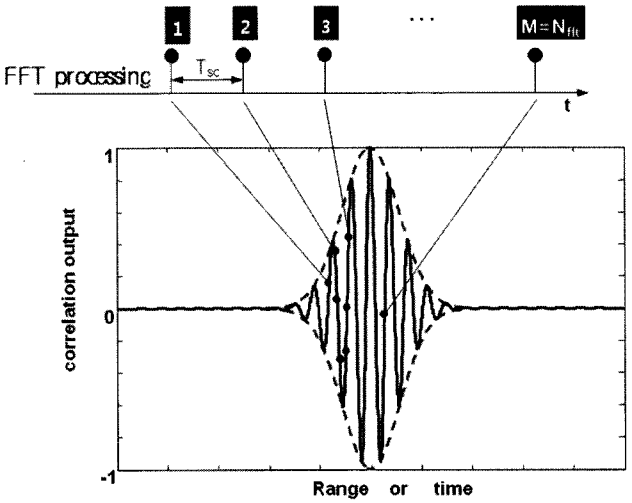

(b) Output signal of sub-correlator

Fig. 5. Concept of sub-correlation and Doppler processing.

tor output data(M-points) and performing the FFT processing provides the Doppler information about the target in the specified range bin. By applying this operation to all delay elements, target information for all range and velocity bins can be obtained.

2-6 Modulation Schemes

There are many modulation types that can generate true random noise signals, these include random AM (Amplitude Modulation), random PM(Phase Modulation), and random FM(Frequency Modulation). A random AM scheme seems to be simple, but it has the following drawbacks: one is the difficulty in implementing wideband signals, another is the non-linear operation(saturation) of the amplifier due to randomly generated high amplitude points, and the other is the need for an extra spectrum-shaping circuit such as a Gaussian filter. Circumventing the above mentioned drawbacks, a random FM scheme can be used. By applying a white Gaussian noise signal with a DC offset to a tuning port of a voltage controlled oscillator(VCO), a random FM noise signal can be efficiently generated, and the required center frequency and bandwidth can be easily controlled by properly adjusting the DC level and amplitude of the tuning noise signal. What is worth noting is that the output frequency is controlled not by the frequency but by the voltage level of the tuning signal. Therefore, a wideband random noise signal is not needed for wideband frequency tuning. Since the Gaussian spectrum can be inherently obtained, designing an absorptive Gaussian filter is not needed. In addition, since the amplitude of the generated random FM signal becomes uniform theoretically, it is nearly free from the problem of the saturation phenomena in nonlinear active devices that generally appears in the random AM scheme.

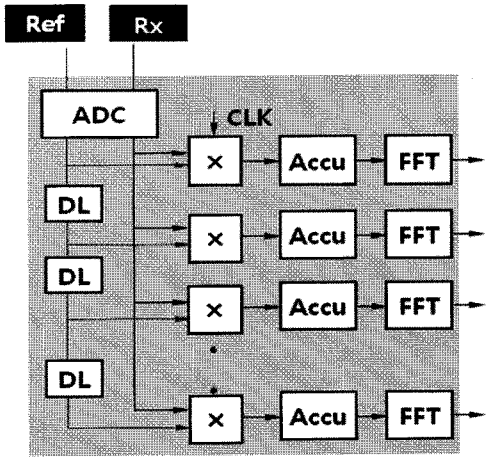

Fig. 6. Block diagram of range and velocity processing by using digital correlator.

2-7 Tx/Rx Isolation Characteristics

In a CW random noise radar system, two separate antennas are generally used for solving a Tx/Rx antenna coupling problem. However, its coupling cannot be removed perfectly. As shown in Fig. 7, the leakage power (N_{leak}) at the Rx terminal can be represented in terms of Tx power(P_{tx}) and antenna isolation(I) as

$$N_{leak} = \frac{P_{tx}}{I} \tag{17}$$

Since this leakage is independent of the thermal noise at the Rx terminal, the total noise power(N_t) becomes

$$N_t = N_{eq} + N_{leak} \tag{18}$$

and its effect can be regarded as an additional loss (leakage loss L_{leak}):

$$L_{leak} = \frac{N_{eq} + N_{leak}}{N_{eq}} = 1 + \frac{N_{leak}}{N_{eq}} \tag{19}$$

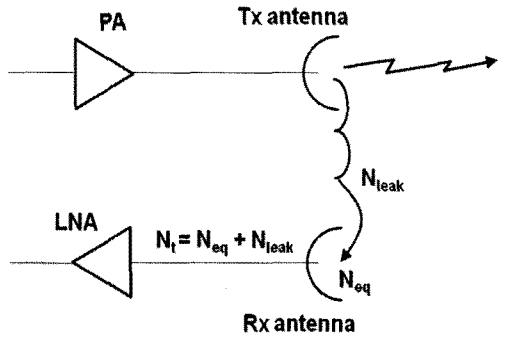

Fig. 7. Analysis of the effect of Tx leakage on the system performance.

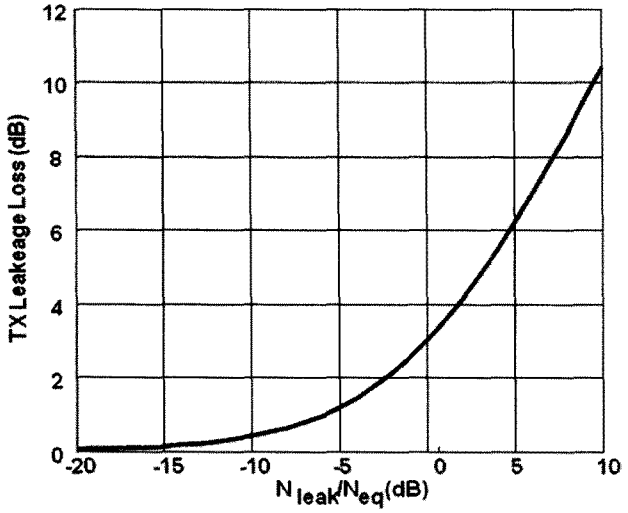

Fig. 8. Additional system loss due to a Tx leakage.

Fig. 8 shows the relation between the leakage loss and the relative leakage power to the equivalent input noise power.

2-8 Range Equation

Finally the radar range equation of the random noise radar is derived and expressed in different but equivalent formulas as

$$R_{\max} = \left[\frac{P_t G_T G_R \lambda^2 \sigma}{(4\pi)^3 k T_0 F_n B_{FFT} L D_x}\right]^{1/4} = \left[\frac{P_t G_T G_R \lambda^2 \sigma T_{\text{int}}}{(4\pi)^3 k T_0 F_n L D_x}\right]^{1/4} = \left[\frac{P_t G_T G_R \lambda^2 \sigma}{(4\pi)^3 k T_0 F_n B L D_x} G_c\right]^{1/4} \quad (20)$$

where the related parameters have the following meanings:

$R_{\max}$: maximum detection range(m)
P_t : Tx power(W)
G_T, G_R : antenna gain of Tx and Rx antennas
λ : wavelength of Tx signal(m)
B_{FFT} : FFT resolution bandwidth(Hz)
B : bandwidth of Tx signal(Hz)
σ : target RCS(m^2)
G_c : correlation gain
T_{int} : integration time for correlation(s)
k : Boltzmann constant[k=1.38*10^{-23} W/(KHz)]
T_0 : absolute temperature(K)
F_n : noise figure of receiver
L : system loss
D_x : detectability factor

In the above equation, the following relations are used for deriving the equivalent expressions

$$B_{FFT} = \Delta f = \frac{1}{T_{\text{int}}} \quad \text{and} \quad G_c = \frac{B}{B_{FFT}} = BT_{\text{int}} \quad (21)$$

and it is known that the performance of the random noise radar is enhanced by the factor of the correlation gain(G_c).

III. Design of Noise Radar System

3-1 System Design

Based on the described design theory, a K-band true random noise radar system was designed for moving target detection. It is well known that Doppler shift is a linear function of the Tx frequency as $f_d = (2v/c) f_0$. Therefore a Tx frequency of K-band results in a higher Doppler frequency shift than the C- or X-band, and it makes Doppler processing relatively easy because the low-frequency interference components can be easily removed. Table 1 lists all the required operational specifications. Since detailed angle processing is not a topic of this feasibility study, the resolution characteristics are not given. The detailed block diagram of the designed radar system is depicted in Fig. 9. Two separated identical antennas with azimuth and elevation beamwidth of 30° and 20°, respectively, were placed for the Tx and Rx uses. The antenna gain is therefore expected to be approximately 17.3 dBi. From the specified range resolution, a Tx bandwidth of 100 MHz is chosen. From the conditions(18), the integration time T_{int} is set to be 2.62 ms, and it results in a correlation gain of 54.19 dB.

Considering the availability of a commercial LNA (low noise amplifier), a noise figure of 3 dB is assumed, and the total system loss is estimated as 6.16 dB(2 way Tx/Rx transmission line loss of 2 dB, correlation and signal processing loss of 2 dB, and Tx/Rx leakage loss of 0.16 dB, some margin of 2 dB). For such a low Tx/Rx leakage loss of 0.16 dB, a Tx/Rx isolation of 120

Table 1. Required operating characteristics.

Parameters		Value	CC
Frequency	Band	K	
Range (m)	Min	15	
	Max	120	
Velocity (m/s)	Min	100	
	Max	300	
Angle (deg)	Azimuth	30	
	Elevation	20	
Resolution	Range(m)	1.5	
	Velocity(m/s)	4	
Detection condition	P_d	0.5	
	P_{fa}	10^{-6}	
	Swerling case	1	
	RCS(m^2)	0.01	

dB should be provided. This amount of isolation can be met by using separate Tx and Rx antennas and coupling cancellation circuit. For the given target fluctuation model(Swerling case), false alarm probability(P_{fa}), and detection probability(P_d), the resulting detectability factor is calculated as 12.77 dB. With these design parameters, it is known that the required minimum Tx power is 14.77 dBm(30 mW) for the specified maximum detection range. Table 2 shows the final design parameters.

3-2 Transmitter with Noise Source

For a practical implementation, a C-band random FM noise signal whose bandwidth is 25 MHz was generated from a VCO which is tuned by an offset narrow-band noise signal. Then this signal is fed into a quadruple multiplier and a BPF successively to obtain a bandwidth of 100 MHz. A signal for reference is coupled from the directional coupler which is placed after PA(Power Amplifier). The final K-band signal is radiated into the coverage space via the Tx antenna.

3-3 Antenna

Two identical antennas were used for both Tx and Rx purposes. A modified waveguide horn array antenna with non-uniform distribution in the E-plane was designed for low sidelobe characteristics. For this purpose, the waveguide is divided into four parts, and one end of each part was fed by a tapered slot structure for wideband operation. Coupling from a non-uniform microstrip feed

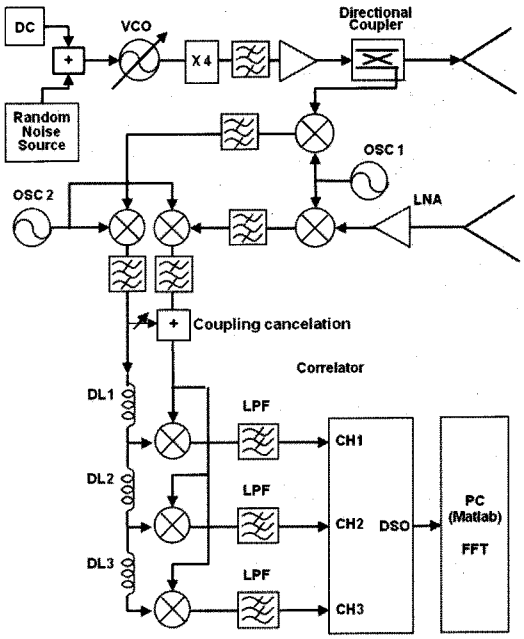

Fig. 9. Block diagram of designed true random noise radar system.

Table 2. Final design parameters.

Parameters	Value	
Tx power(dBm)	14.77	30 mW
B(MHz)	100.00	
Antenna gain(dBi)	17.30	
T_{int}(ms)	4.27	
Noise figure(dB)	3.00	
System loss(dB)	6.16	
Detectability factor(dB)	12.77	
R_{max}(m)	147.51	
ΔR(m)	1.5	
v_{max}(m/s)	1,500	
Δv(m/s)	1.46	

network to the tapered slots was attained by microstrip to slotline transitions. Fig. 10(a) shows the fabricated antenna, and the measured return loss and radiation pattern characteristics are shown in Fig. 10(b). The measured beamwidth in the E- and H-planes of the designed antenna were 20.3 and 30.5 degrees respectively, and the measured antenna gain was almost 17.5 dBi, which shows good agreement with the specifications. Fig. 11 depicts the measured isolation data between the Tx and Rx antennas as a function of spacing (center to center) along with the simulation results[10], and isolation over

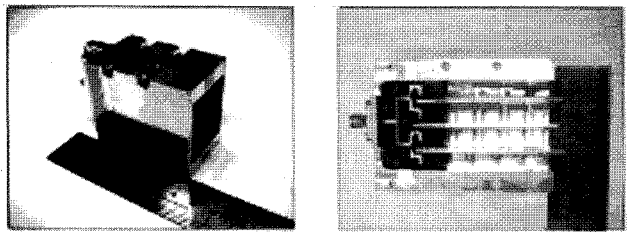

(a) Fabricated antenna

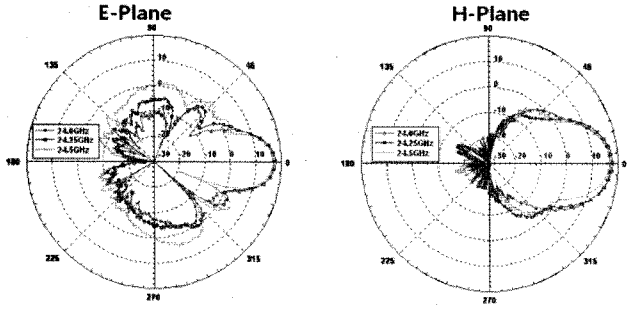

(b) Measured results of E- and H-plane patterns

Fig. 10. Measured pattern characteristics of the fabricated antenna.

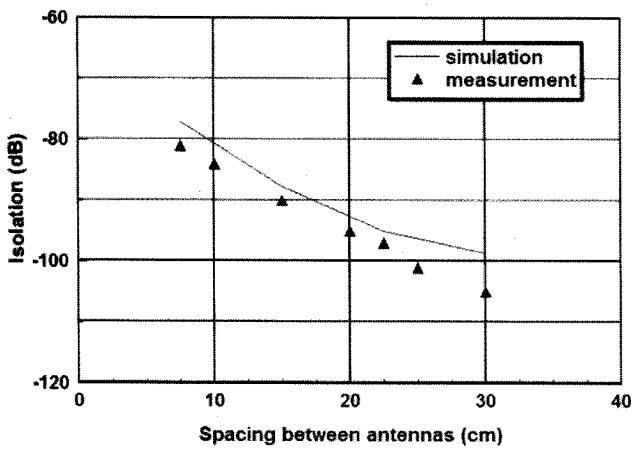

Fig. 11. Measured isolation between Tx/Rx antennas.

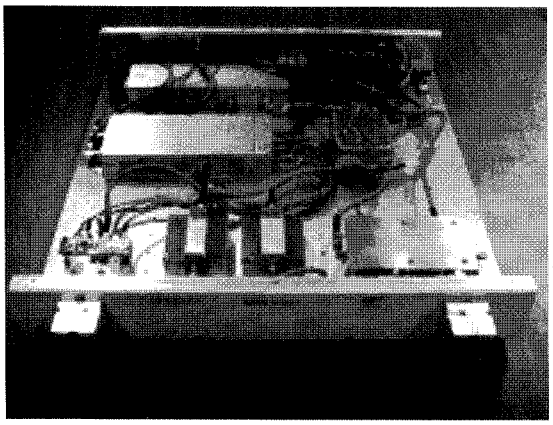

Fig. 12. Implemented noise radar system.

100 dB is guaranteed when the spacing is kept 25 cm apart. An Additional 20.5 dB isolation was attained by a coupling cancellation circuit in the IF stage.

3-4 Receiver and Correlator

The received signal is amplified in an LNA to enhance the system sensitivity. For easy correlation and Doppler processing, the amplified Rx signal and the delayed reference signals are down converted(double down-conversion). Since the aim of this paper is a feasibility study for implementing a noise radar system, a multi- channel analog correlator consisting of mixers, delay lines with different delay time, and LPFs was adopted to extract the target information.

Ⅳ. Experimental Results and Discussion

4-1 Range Calibration

The implemented noise radar system is shown in Fig. 13. For the range calibration of the implemented noise radar system, a simple but efficient double-spectral processing[11] technique was used. The frequency spectrum of the sum of Tx signal $x_t(t)$ and Rx signal $x_t\ (t-\tau_0)$ from the fixed target can be written as

$$|Y(f)| = |X_t(f)||1+e^{-j\omega\tau_0}| \tag{22}$$

Since the time delay can be determined from the measured period of the spectrum of $|Y(f)|$ in the spectrum analyzer, the target range can be easily calculated. The experimental setup for the range calibration is shown in Fig. 14, where a coaxial line with a propagation delay time of 34 ns was connected between the Tx output and Rx input ports. The calculated delay time from the measured period of spectrum was 38.5 ns. Compensation with 4.5 ns delay time(0.675 m range) is therefore needed for the precise range information processing.

4-2 Detection of Moving Targets

Due to the lack of an experimental setup for full verification of the performance of the developed random noise radar, performances of the range and velocity processing were checked with two experiments. Others were verified by calculation from the measured data of related parameters.

The first experiment was performed with a moving bicycle. Even though the expected velocity of the target (4.5 m/s) is far below from the range of specification, the experiment is very meaningful for checking the basic operations. Fig. 14 shows the test setup with a bi-

cycle moving toward the antenna. Three parallel connected delayed reference channels were made with different delay times of 30 ns(4.5 m), 40 ns(6 m), and 50 ns(7.5 m), respectively. Since the estimated Doppler shift is 0.72 kHz, LPFs with a cutoff frequency of 1.2 kHz were chosen as sub-correlators. A trigger circuit was made to generate a signal for data logging when the target passes the line which is 15.5 m apart from the antenna. Thus the estimated time for the correlation peaks are 1.78 sec(range bin of 7.5 m), 2.11 sec(range bin of 6 m), and 2.44 sec(range bin of 4.5 m), respectively.

The outputs of three connected to three different channels(CH1, CH2, and CH3) of a digital storage oscilloscope(DSO) for data logging, where the sampling frequency of 9.6 kHz(8 times higher than the cutoff frequency) was chosen. Then 2048-point FFT processing, which corresponds to T_{int}=0.213 sec, was conducted in the Matlab environment[9] with the logging data. The attainable velocity resolution becomes 0.03 m/s. The original data in the measurement-time domain are displayed in Fig 15, and the measured delay-time(range) data of the

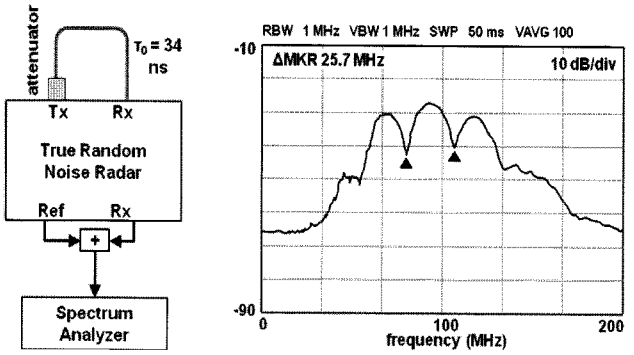

Fig. 13. Experimental setup for double spectral processing and measurement result.

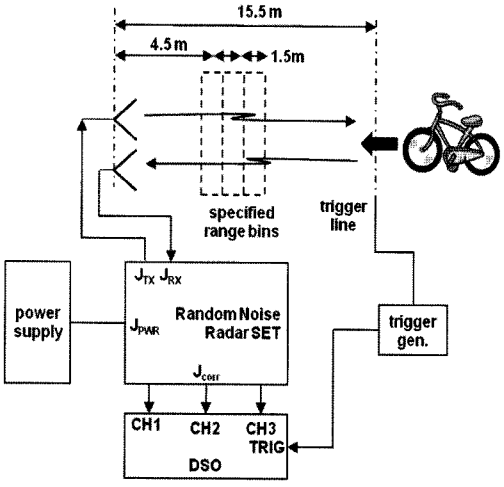

Fig. 14. Measurement setup for range and velocity processing by using bicycle as a moving target.

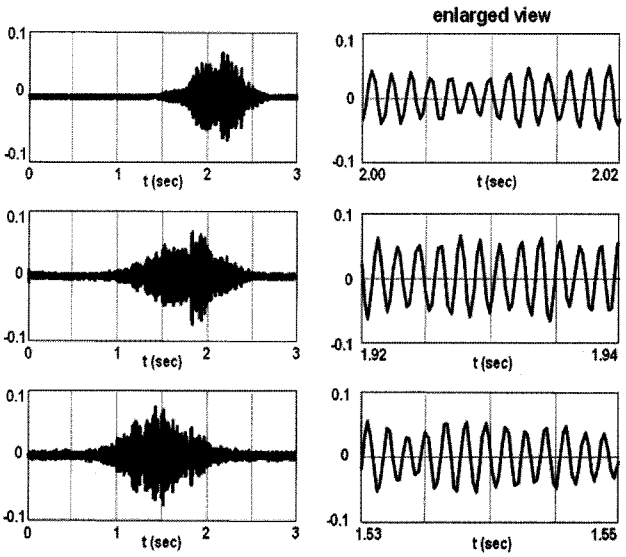

Fig. 15. Correlation integral results at each channel, and its enlarged view.

moving target show reasonable agreement with the expected data. The average pulse width of 0.55 sec corresponds to the width in the range of 0.59 sec × 4.45 m/s=2.63 m. Considering the effective length of the bicycle(about 1.1 m), the range resolution for a point target can therefore be reasonably estimated to be 1.43 m, which is very close to the specification. The average velocity information obtained from the measured Doppler frequencies is 4.45 m/s, which also agrees well with the expected moving speed of the bicycle.

Next, the main experiment was conducted with a small but high-speed target. In this case, LPFs with cutoff frequency of 60 kHz were used since the expected maximum Doppler shift for a target with v=300 m/s

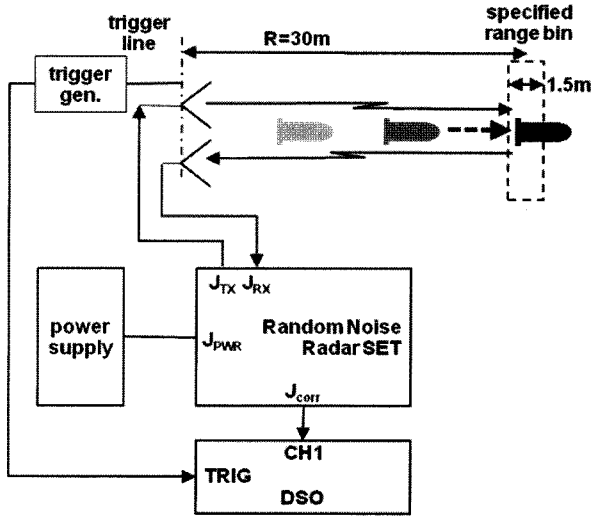

Fig. 16. Measurement setup for range and velocity processing by using small sized but high speed target.

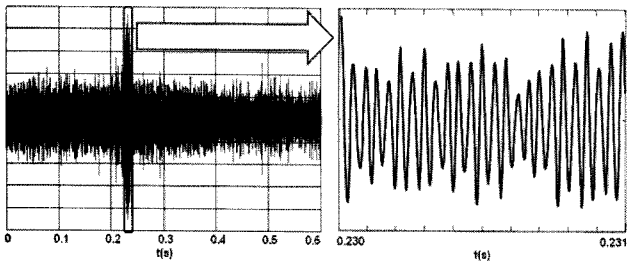

Fig. 17. Detection result of high speed target(150 m/s).

target was 48 kHz. The sampling frequency for data logging was set to be 480 kHz(8 times higher than the cutoff frequency). The speed of the target used in the experiment was reported to be approximately 150 m/s. A coaxial cable with 200 ns delay was inserted in the delayed reference channel for monitoring the range bin of 30 m(measurement delay time of 0.2 sec). The test setup for this experiment is shown in Fig. 16, where the same trigger signal was used for firing the target and data logging. There was an approximate firing delay of 0.03 sec, thus the estimated time for the correlation peak is about 0.23 sec. As shown in Fig. 17, the obtained measurement time for the peak correlation agrees well with the expected. By FFT processing with 2048-point data, the velocity information was obtained as 152.85 m/s showing close agreement with the expected results. In this case, the integration time becomes T_{int}=4.27 ms, and the attainable velocity resolution is 2.46 m/s. All the results of the experiments reasonably validate the design and implementation of the random-noise radar system.

V. Conclusion

The design theory and experimental results of a true random noise radar system were presented. Target range information can be extracted precisely by correlation processing between the delayed reference and the signal received from targets, and the velocity information by Doppler processing with successive correlation data. A K-band noise radar system was designed using a random FM noise signal, and the characteristics of the fabricated system were examined with the laboratory and outdoor experiments. A C-band random FM noise signal was generated by applying a low-frequency white Gaussian noise source to a VCO(voltage controlled oscillator), and a K-band TX noise signal with 100 MHz bandwidth was obtained by using a following frequency multiplier. Modified waveguide horn arrays were designed and fabricated, and used for Tx and Rx antennas, and the required amount of Tx/Rx isolation was attained by using a coupling cancellation circuit as well as keeping them apart with predetermined spacing. A double down-conversion scheme was used in both the Rx and the reference channels, respectively, for easy post processing such as correlation and Doppler processing. The implemented noise radar was calibrated by applying the double spectral processing. Then the performance was examined with a moving bicycle and a very high-speed target with velocity of 150 m/s, and the results extracted with the Matlab simulation with the logging data were found to be in reasonable agreement with the expected ones.

To the authors' knowledge, the digital correlator can be implemented by using the state-of-art technology with an elaborate design. Research on the digital correlator including the implementation and algorithm study is our future work.

Due to the randomness of true noise signals, various random noise radar systems are very promising candidates for simultaneous operation of multiple radar systems in the same zone that are needed in active protection of important facilities and automobile collision avoidance. In addition, LPI characteristics make noise radar very suitable for use in the future electronic warfare environment.

This research was supported by National Research Foundation(NRF) of Korea Grant funded by the Korean Government(MEST) (No. F01-2007-000-10216-0).

References

[1] B. M. Horton, "Noise-modulated distance measuring system", *Proc. IRE*, vol. 47, no. 5, pp. 821-828, May 1959.

[2] L. Liuguosui, S. Xiangquan, L. Jinhui, Y. Guoyu, and S. Yaoliang, "Design of noise FM-CW radar and its implementation", *IEEE. Proc.-F*, vol. 138, no. 5, pp. 420-426, Oct. 1991.

[3] K. A. Lukin, "Millimeter wave noise radar applications: Theory and experiment", *IEEE MSMW 2001, Symp. Proc.*, Kharkov, Ukraine, pp. 68-73, Jun. 2001.

[4] M. Dawood, R. M. Narayanan, "Receiver characteristics for the coherent UWB random noise radar", *IEEE Trans. Aerospace and Electronic Systems*, vol. 37, no. 2, pp. 586-594, Apr. 2001.

[5] S. R. J. Axellson, "Noise radar using random phase and frequency modulation", *IEEE Trans. Geoscience and Remote Sensing*, vol. 42, no. 11, pp. 2370-2384, Nov. 2004.

[6] K. A. Lukin, "Noise radar technology: the principles and short overview", *Applied Radio Electronics*, Kharkov, IRE NAS of Ukraine, vol. 4, no. 1, pp.

74-79, Feb. 2005.
[7] J. S. Bendat, A. G. Piersol, *Engineering Applications of Correlation and Spectral Analysis*, 2nd Ed., Wiley, 1993.
[8] Matlab 2007a, Mathworks, MA 01760-2098, USA.
[9] FEKO 5.3, EM software and Systems, South Africa.
[10] V. I. Kalinin, "Ultra-wideband data transmission with double spectral processing of noise waveforms", *Technical Physics Letters*, vol. 31, no. 11, pp. 929-931, Nov. 2005.

Woo-Ki Min

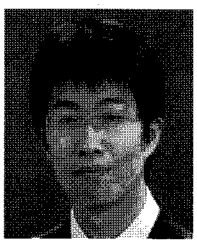

received the B.S. degree in 2008, and is currently working toward the M.S. degree in the School of Electronic Engineering, Chung-Ang University. His research interests include the design of RF and microwave circuits, antennas, and radar systems.

Cheol-Hoo Kim

received the B.S., and M.S. degree in electronic engineering from Kyungpook National Uuniversity, Deagu, Korea in 1987 and 1989, respectively. He is currently working toward the Ph.D. degree in the School of Electronic Engineering, Chung-Ang University, Seoul, Korea. From 1989 to 1994, he had worked for LG Innotek (LIG Nex1). From 1994 for Samsung Electronics for 5 years. Since 2000, he has been working at MTI Co., LTD. His research interests include the design of wireless communication and radar systems.

Constantin A. Lukin

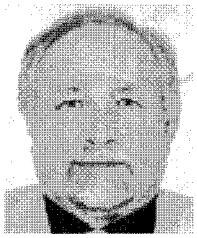

received the B.S. degree in the Kharkov State University, Ukraine in 1973, his Candidate of Sciences degree in the Moscow State University, Russia in 1980, his Doctor of Science degree in the Kharkov State University, Ukraine in 1989. Since 1973, he has been working at IRE NASU, Ukraine, where he is currently a Head of LNDES. His research interests are in the areas of Nonlinear dynamics and applications to chaos and random noise signals, radar systems for SAR and surveillance.

Jeong-Phill Kim

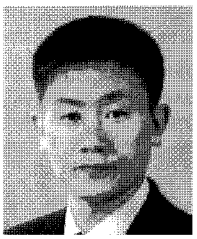

received the B.S. degree from Seoul National University, Seoul, Korea in 1988, his M.S. and Ph.D. degrees from POSTECH, Pohang, Korea in 1990 and 1998, respectively, all in electronic engineering. From 1990 to 2001, he had worked for LG Innotek(LIG Nex1). Now he is with the School of Electronic Engineering, Chung-Ang University as an associate professor. His research interests include the design of microwave circuits and antenna, wireless communication and radar systems, especially in the random noise radar system.